THE ASTROPHYSICAL JOURNAL, 419:311–317, 1993 December 10

DYNAMICALLY COMPTONIZED SPECTRA FROM NEAR-CRITICAL ACCRETION ONTO NEUTRON STARS

LUCA ZAMPIERI
International School for Advanced Studies, Trieste, Via Beirut 2-4, 34014 Miramare-Trieste, Italy
ROBERTO TUROLLA
Department of Physics, University of Padova, Via Marzolo 8, 35131 Padova, Italy
AND
ALDO TREVES
International School for Advanced Studies, Trieste, Via Beirut 2-4, 34014 Miramare-Trieste, Italy
Received 1993 March 17; accepted 1993 June 17

ABSTRACT

We investigate the effects of dynamical Comptonization on the emergent radiation spectrum produced by near-critical accretion onto a neutron star. The flow dynamics and the transfer of radiation are self-consistently solved in the case of a spherically symmetric, "cold," pure scattering flow, including general relativity. A sequence of models, each characterized by the value of the total observed luminosity, was obtained assuming that the spectrum at the star surface is blackbody in shape. It is found that when the luminosity approaches the Eddington limit dynamical effects become important shifting the spectrum to the blue and producing a power-law, high-energy tail. The relevance of these results in connection with the observed spectral properties of LMXBs, and of Cyg X-2 in particular, are discussed.

Subject headings: accretion, accretion disks — binaries: close — radiative transfer — stars: individual (Cygnus X-2) — stars: neutron

1. INTRODUCTION

Most of the bright X-rays sources in the Galaxy are close binary systems containing an accreting neutron star. In several cases the neutron star manifests through a regular periodicity (X-ray pulsators), which is related to the high magnetic field ($B \sim 10^{12}$ G) endowed by the rotating neutron star. However, in the great majority of the so-called low-mass X-ray binaries (LMXBs), no regular modulation is present, and the neutron star magnetic field may be orders of magnitudes below that of X-ray pulsators. In this case, the dynamics of accretion onto the neutron star may be practically unaffected by the magnetic field.

Observationally the spectrum of LMXBs is rather complex and is characterized by a drop in the flux above 6–10 keV, which contrasts with the substantially harder emission of X-ray pulsators; in some sources, however, a steep power-law tail above 20 keV is observed (see, e.g., Maurer et al. 1982; Matt et al. 1990 and references therein). Fitting the observed spectra requires the superposition of a number of simple laws, like a thin bremsstrahlung plus a blackbody, or a bremsstrahlung plus a power law, or a multitemperature blackbody disk plus a boundary layer blackbody, or a Comptonized spectrum. Since LMXBs are variable, their emission can be characterized by X-ray intensity-color and color-color relations which also have been studied in detail in connection with the so-called quasi-periodic oscillations observed in a number of these sources (see, e.g., van der Klis 1989). Basically, one finds states in which the X-ray hardness ratio increases with the X-ray intensity and states where it is substantially constant, although the actual behavior is much more complicated. The total luminosity is, in some cases, a large fraction of the Eddington limit for a solar mass.

While a good fit to the spectral data obviously requires the superposition of various physical regions, each emitting a rather complex spectrum, it seems of interest to construct simple models, physically well defined, which can shed light on some aspects of the formation of the spectrum and be part of the overall picture.

In this spirit we consider here a spherically accreting, unmagnetized neutron star which radiates close to the Eddington limit. The hydrodynamics corresponding to such a picture was studied by Maraschi, Reina, & Treves (1974, 1978), who found the noticeable result that for high luminosities the infall velocity, approaching the star, reaches a maximum and then starts to decrease, owing to the pressure exerted by radiation; a settling regime is established above the neutron star surface. This problem was reexamined by Miller (1990) and Park & Miller (1991), who included also general relativity and obtained very similar results.

Radiation interacts with the inflowing gas and, even in the absence of emission processes, the emergent spectrum can be modified by dynamical Comptonization due to bulk motion (Blandford & Payne 1981a, b; Payne & Blandford 1981 [hereafter PB]; Colpi 1988). The effects of dynamical Comptonization in accretion onto neutron stars were recently investigated by Mastichiadis & Kylafis (1992, hereafter MK). Their results, however, were obtained using an assigned, power-law velocity profile, which is a poor approximation when the luminosity is close to the Eddington limit, and they are valid only in the diffusion regime.

In this paper we present self-consistent solutions for the transfer of radiation in accreting flows onto a neutron star. General-relativistic radiative transfer is tackled using projected symmetric trace-free (PSTF) moment formalism (Thorne 1981;

Turolla & Nobili 1988; Nobili, Turolla, & Zampieri 1993). In order to explore the effects of dynamics and gravity, we treat just the pure scattering case and assume that photons are generated at the neutron star surface with a Planckian spectral distribution.

The plan of the paper is the following. In § 2 we discuss the equations governing the gas dynamics and the transfer of radiation while the results of numerical integration are presented in § 3. Section 4 is devoted to a comparison of our models with the observed spectral properties of LMXBs.

2. THE MODEL

We assume that X-ray radiation observed in LMXBs is generated by the conversion of gravitational potential energy, as matter is spherically accreted onto a slowly rotating, weakly magnetized neutron star. If the flow velocity vanishes at the neutron star surface, the efficiency of the accretion process is given by the variation of the specific gravitational energy E_p

$$\epsilon = (E_p)_\infty - (E_p)_* = 1 - (\sqrt{-g_{00}})_* = 1 - \sqrt{1 - \frac{2GM_*}{c^2 R_*}} \sim \frac{GM_*}{c^2 R_*}, \quad (1)$$

where M_* and R_* denote the neutron star mass and radius, respectively, and we used a vacuum Schwarzschild solution to describe the gravitational field outside the star. By introducing the adimensional radial coordinate $r = R/R_g$, $R_g = 2GM_*/c^2$, and the accretion rate $\dot{M}$, the total luminosity observed at infinity is

$$L_\infty = \epsilon \dot{M} c^2 = \left(1 - \sqrt{1 - \frac{1}{r_*}}\right) \dot{M} c^2 . \quad (2)$$

The complete analysis of a steady state, spherically symmetric gas flow onto a compact star is a complex task since the appearance of shocks and/or of a boundary layer at the neutron star surface should be expected. However, some reasonable simplifying assumptions can be made if one is not interested in treating in detail the inner accretion layer where nearly all the energy is released. First of all, we note that $\epsilon \sim 0.1$ for $M_* \sim 1.5\ M_\odot$ and $R_* \sim 10$ km, so that $L_\infty/L_E = l_\infty \sim 1$ if $\dot{M}/\dot{M}_E = \dot{m} \sim 1$, where $L_E = 4\pi G M_* c/\kappa_{es}$ is the Eddington luminosity and $\dot{M}_E = L_E/c^2$ is the critical accretion rate. By comparing this value for l_∞ with the maximal luminosity attainable in black hole accretion, $l_{BH} \lesssim 0.01$ (see Nobili, Turolla, & Zampieri 1991), it follows that the infalling gas can radiate, at most, a few percent of the total energy output before the impact with the surface of the star. We can therefore safely neglect emission processes in the accreting gas and treat the material as a pure scattering medium. In this hypothesis the radiation spectrum observed at infinity is formed in the boundary layer by processes which are not important to specify in detail, since the overall spectral properties are determined mainly by scatterings as radiation propagates outward. The main goal of our investigation is to study the effects of dynamics on radiative transfer, and therefore we consider only coherent (Thomson) scattering. We make the further assumption that the plasma is "cold," in the sense that its enthalpy is always much less than effective gravity. This is equivalent to say that the gas velocity is everywhere greater than the sound speed, $v > v_s$, and limits the validity of our approach to the supersonic part of the flow.

For a recent derivation of the equations governing the dynamics of the matter gas and the transfer of radiation in spherical, stationary accretion in a Schwarzschild gravitational field we refer to Nobili et al. (1991). In the case of a "cold," pure scattering plasma they reduce to the form

$$v^2 \frac{(yv)'}{yv} = -\frac{1}{2y^2 r} + \frac{4\pi \kappa_{es} r R_g}{yc^2} H , \quad (3)$$

$$2\kappa_{es} R_g r^2 \varrho v y = \dot{m} , \quad (4)$$

$$H' - vJ' + 2H\left(1 + \frac{y'}{y}\right) - vJ\left\{f\left[\frac{(yv)'}{yv} - 1\right] + \frac{4}{3}\left[\frac{(yv)'}{yv} + 2\right]\right\} = 0 \quad (5a)$$

$$\left(f + \frac{1}{3}\right)J' - vH' + \left[f' + f\left(3 + \frac{y'}{y}\right) + \frac{4}{3}\frac{y'}{y}\right]J - 2vH\left[\frac{(yv)'}{yv} + 1\right] = -\frac{\kappa_{es} r R_g \varrho H}{y} . \quad (5b)$$

Here v is in units of c, $y = [(1 - 1/r)/(1 - v^2)]^{1/2}$, a prime denotes derivation with respect to $\ln r$ and J and H are the radiation energy density and flux, as measured in the local rest frame (LRF) of the fluid; the comoving luminosity L is related to H by $L = 16\pi^2 r^2 R_g^2 cH$, where an extra c factor appears because all moments are in ergs^{-1} cm^{-3}. The variable Eddington factor, $f = K/J - \frac{1}{3}$ is a given function of the optical depth τ of the form

$$f(\tau) = \frac{2}{3(1 + \tau^2)} . \quad (6)$$

The solution of equations (3)–(5) provides the velocity and density profiles of the matter gas and the radial evolution of the frequency-integrated moments, once boundary conditions are given. In treating a pure scattering problem one of the conditions must fix the value of either the radiation energy density or of the flux at some radius. Computed models were obtained assigning the value of the luminosity far from the star. Since M_* and R_* are known, equation (2) gives immediately the accretion rate, while the two remaining boundary conditions are

$$J = H , \quad r = r_{out} , \quad \text{(radial streaming)} ;$$

$$v = \sqrt{\frac{1 - l_\infty}{r}} ; \quad r = r_{out} ; \quad \text{("modified" free fall)} .$$

It should be noted that l_∞ is the only free parameter of the model.

The results of numerical integrations are shown in Figures 1 and 2, for two representative values of l_∞, $l_\infty = 0.3$, and $l_\infty = 0.9$, respectively; in all models $M_* = 1.4\ M_\odot$ and $R_* = 10$ km. The settling regime is a common feature of all high-luminosity solutions and is clearly visible in Figure 2*b*. The overall behavior of our models is close to that found by Maraschi et al. (1978), Miller (1990), and Park & Miller (1991) under quite similar assumptions.

The self-consistent velocity and density profiles obtained from the simultaneous integration of the hydrodynamical and frequency-integrated moment equations can now be used to solve the full, frequency-dependent transfer problem. The frequency-dependent version of equations (5) is (Thorne 1981;

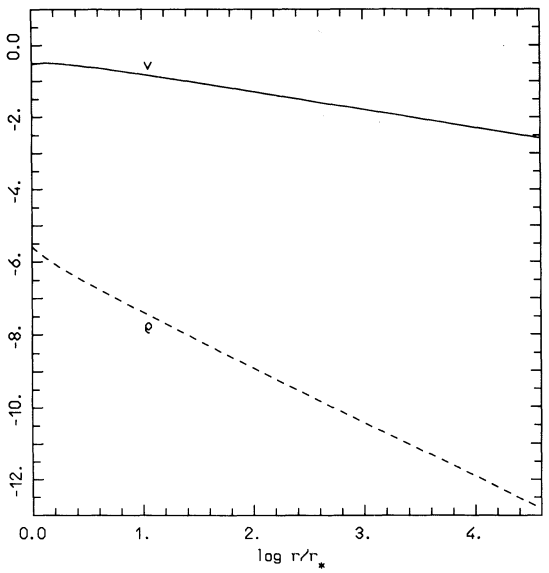

FIG. 1a

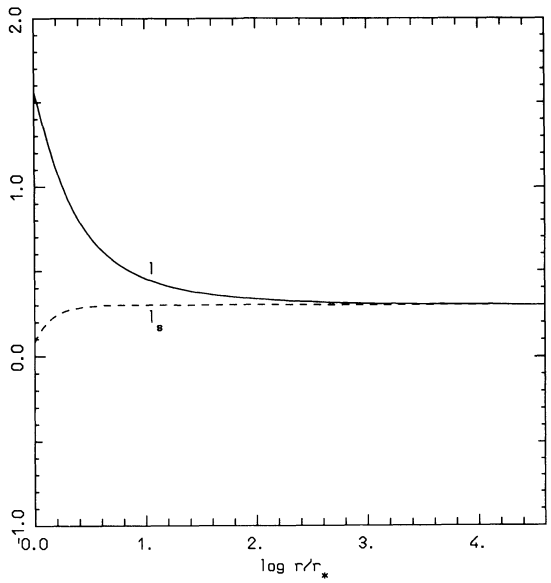

FIG. 1b

FIG. 1.—(*a*) Velocity and density profiles vs. radius for the model with $l_\infty = 0.3$. Scales are logarithmic and density is in g cm^{-3}. (*b*) Stationary, l_s, and comoving, l, luminosities for the model with $l_\infty = 0.3$.

Nobili et al. 1993)

$$\frac{\partial H_\nu}{\partial \ln r} + 2H_\nu + \frac{y'}{y}\left(H_\nu - \frac{\partial H_\nu}{\partial \ln \nu}\right) - v\left\{\frac{\partial J_\nu}{\partial \ln r} + (\beta+2)J_\nu - \left[f(\beta-1) - \frac{1}{3}(\beta+2)\right]\frac{\partial J_\nu}{\partial \ln \nu}\right\} = 0\,, \quad (7a)$$

$$\left(f+\frac{1}{3}\right)\frac{\partial J_\nu}{\partial \ln r} + f\left(3+\frac{f'}{f}\right)J_\nu + \frac{y'}{y}\left[J_\nu + \left(f+\frac{1}{3}\right)\frac{\partial J_\nu}{\partial \ln \nu}\right] - v\left[\frac{\partial H_\nu}{\partial \ln r} + \frac{1}{5}(7\beta+8)H_\nu - \frac{1}{5}(3\beta+2)\frac{\partial H_\nu}{\partial \ln \nu}\right] - g(\beta-1)\left(H_\nu + \frac{\partial H_\nu}{\partial \ln \nu}\right) = -\frac{\kappa_{es}\varrho r R_g H_\nu}{y}\,, \quad (7b)$$

where $\beta = (yv)'/(yv)$ and the index ν denotes frequency-dependent quantities. In writing equations (7) we have assumed that the Eddington factors f and $g = N/H - 3/5$ are independent of frequency; actually, f is given again by equation (6) and $g = 3f/5$.

Equations (7) have to be solved as a two points boundary value problem in space and an initial value problem in frequency. In our particular case, we have assigned the flux spectral distribution at the star surface

$$H_\nu(r_*) = \bar{H}_\nu\,,$$

with the additional constraint that

$$\int_0^\infty \bar{H}_\nu\, d\nu = H(r_*)\,, \quad (8)$$

where $H(r_*)$ is the frequency-integrated flux at r_*, as given by the solution of equations (3)–(5); the remaining radial condition is again

$$J_\nu = H_\nu\,, \quad r = r_{\rm out} \quad \text{(radial streaming)}\,.$$

A detailed discussion of the form of the input spectrum, together with the choice of the frequency conditions, is postponed to the next section. Here we want to show that dynamical effects on radiative transfer are going to be relevant in our models. As discussed by Payne & Blandford (1981) and Nobili et al. (1993), bulk motion Comptonization is expected to become important in regions where $\tau > 1$ and $\tau v \sim 1$. By making use of equations (2) and (4), neglecting relativistic corrections and assuming $\tau \sim \kappa_{es}\varrho r R_g$, we have that

$$(\tau v)_* \sim \frac{\dot{m}}{2r_*} \sim l_\infty\,, \quad (9)$$

which shows that close to the star surface τv is indeed not far from unity for near critical accretion. Beside this effect, which is not relativistic arising from first-order terms in v, GR corrections are also important, at least when velocity starts to deviate from free fall. In this case, in fact, y, which is very close to unity and nearly constant in free fall, drops below one and photons start to experience a gravitational redshift.

3. RESULTS

In the case of a weakly magnetized neutron star accreting close to the Eddington limit, as we are considering here, we assume that photons are generated only at the surface, through some convenient mechanism that could convert the kinetic energy of the infalling gas into radiation with a given spectral distribution. The simplest choice that can be made is that the input spectrum is Planckian in shape

$$H_x(r_*) = A\,\frac{x^3}{\exp x - 1}\,, \quad (10)$$

$x = h\nu/kT_*$, where the temperature $T_* = T(r_*)$ is fixed by the condition

$$T_* = \left(\frac{L_\infty}{4\pi R_*^2 \sigma}\right)^{1/4}. \quad (11)$$

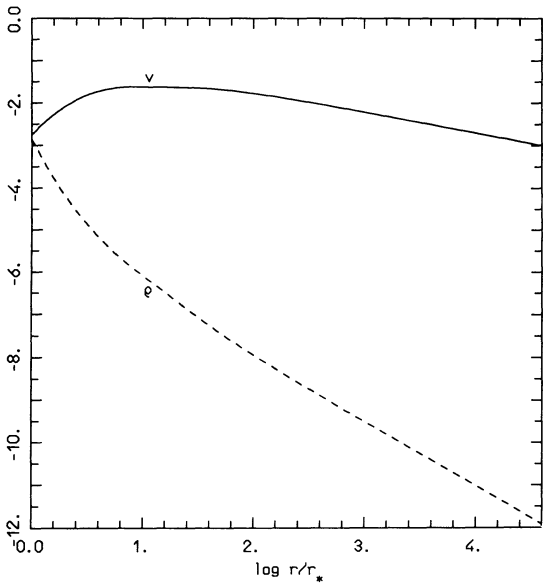

FIG. 2a

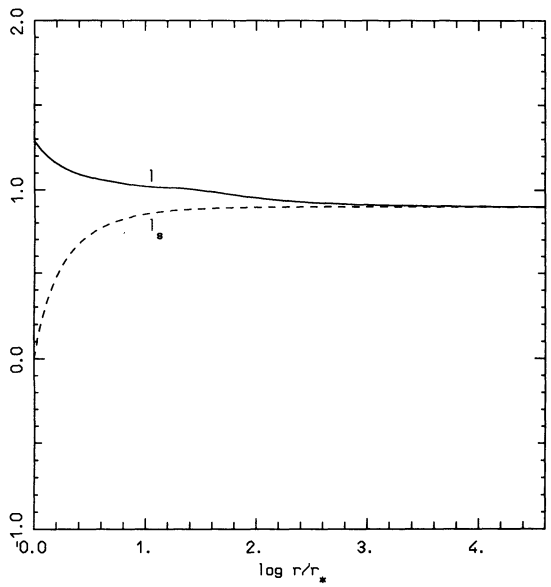

FIG. 2b

FIG. 2.—(*a*) Same as in Fig. 1*a* for the model with $l_\infty = 0.9$. (*b*) Same as in Fig. 1*b* for the model with $l_\infty = 0.9$.

This expression for T_* is justified if the effective optical depth in the flow is always smaller than unity, as indeed should be the case in all our models. The constant A appearing in equation (10) is determined by normalization (8).

The integration of equations (7) was performed using an original numerical code based on a relaxation method (for a detailed discussion, see Nobili et al. 1993). This transfer code was designed to deal with fairly general situations in which dynamics and/or gravity become important and was tested solving a number of simple problems for which analytical solutions were available (Nobili et al. 1993). As a further check on the accuracy of the method in the present case, we compared the integral of the frequency dependent flux with the integrated luminosity at each radius; the largest relative error is some percent. A grid with 30 frequency bins $\times$ 60 radial zones with $0.4 < \log r < 5$ and $-0.5 < \log x < 1.2$ was used.

Two different sets of frequency boundary conditions have been used in the calculations, according to the value of l_∞ which characterizes the model. For models with luminosity $l_\infty \lesssim 0.4$ the spectrum drifts toward low frequencies because gravitational redshift dominates over dynamical Comptonization (see the following discussion), so that both conditions must be specified at the largest frequency mesh point $x_{\max}$

$$\frac{\partial \ln J_x}{\partial \ln x} = \frac{\partial \ln H_x}{\partial \ln x}, \quad x = x_{\max}; \tag{12a}$$

$$\frac{\partial \ln J_x}{\partial \ln x} = 3 - x, \quad x = x_{\max} \quad \text{(Wien law)}. \tag{12b}$$

The situation is reversed for models with luminosity $l_\infty \gtrsim 0.4$ and equations (12a)–(12b) are replaced by

$$\frac{\partial \ln J_x}{\partial \ln x} = \frac{\partial \ln H_x}{\partial \ln x}, \quad x = x_{\min}; \tag{13a}$$

$$\frac{\partial \ln J_x}{\partial \ln x} = 2, \quad x = x_{\min} \quad \text{(Rayleigh-Jeans law)}. \tag{13b}$$

Conditions (12b) and (13b) express the fact that J_x must remain blackbody in shape at high (low) frequencies while conditions (12a) and (13a) derive from the request that $H_x \propto J_x$ in a pure scattering medium. A discussion on how frequency conditions should be placed in solving the transfer problem in moving media can be found in Mihalas, Kusnaz, & Hummer (1976), Nobili et al. (1993), and Turolla et al. (1993). Numerical integrations show that in a small luminosity range around $l_\infty = 0.4$ both sets of boundary conditions work satisfactorily.

Some representative spectra are shown in Figures 3 and 4 and results are summarized in Table 1, where the "soft" and "hard" colors of the emergent spectrum are reported together with count rate in the 1–17 keV energy band; the last column gives the value of the photon spectral index if a power-law tail forms at high energies. The number flux was computed assuming a distance of 8 kpc for the source.

TABLE 1

CHARACTERISTIC PARAMETERS FOR SELECTED MODELS

l_∞	τ_*[a]	$(\tau v)_*$	(3–6)[b] / (1–3)	(6–17)[c] / (3–6)	Count Rate[d]	α[e]
0.1.....	0.3	0.17	0.17	0.02	0.40	...
0.2.....	0.7	0.31	0.31	0.06	0.73	...
0.3.....	1.3	0.37	0.40	0.09	0.96	...
0.4.....	2.2	0.38	0.68	0.20	1.00	...
0.5.....	4.0	0.38	1.06	0.49	0.87	...
0.6.....	7.1	0.39	1.28	0.70	0.86	...
0.7.....	14	0.38	1.44	0.98	0.82	...
0.8.....	33	0.34	1.63	1.23	0.79	3.3
0.9.....	1.8×10^2	0.30	1.79	1.53	0.75	3.4
0.95....	1.2×10^3	0.28	1.87	1.69	0.72	3.5

[a] Electron scattering optical depth at the star surface.
[b] "Soft" color: N_{3-6}/N_{1-3}, where N is the photon count rate in the specified energy range.
[c] "Hard" color: N_{6-17}/N_{3-6}.
[d] Count rate: N_{1-17} (arbitrary units).
[e] Photon spectral index: $-\partial \ln N_\nu / \partial \ln \nu$, calculated above 20 keV.

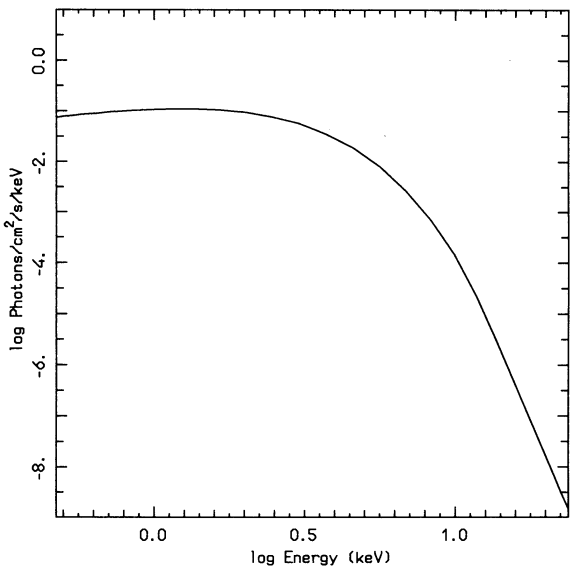

FIG. 3.—Number flux spectral distribution for the model with $l_\infty = 0.3$. The source is assumed to be at a distance of 8 kpc.

As can be clearly seen from the figures, the behavior of the emergent spectrum changes significantly around $l_\infty = 0.4$. For $l_\infty \lesssim 0.4$, in fact, the flow becomes optically thin to scattering and, although $(\tau v)_* \sim 0.3$, bulk motion Comptonization has little effect, because the probability for a photon to scatter before escaping to infinity becomes very low. The fact that $(\tau v)_*$ is not far from unity means that the typical fractional energy change per scattering is still large but electron-photon collisions are so few that the total energy exchange is negligible. Consequently the spectrum at infinity remains nearly Planckian but is rigidly shifted to the red (see Fig. 3) by the effect of gravity. As l_∞ is increased beyond 0.4, models start to develop a thick core, $(\tau v)_*$ remains fairly constant because v_* decreases and τ increases, but now dynamical Comptonization is important owing to the larger optical depth near the stellar surface.

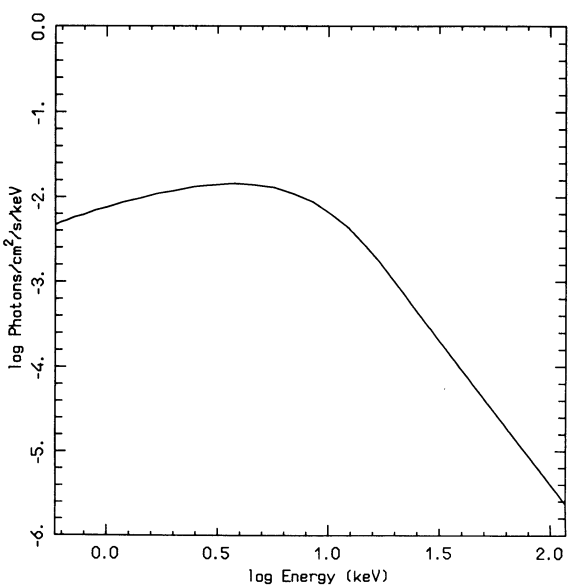

FIG. 4.—Same as in Fig. 3 for the model with $l_\infty = 0.9$

The emergent spectrum is systematically shifted to the blue and a power-law, high-energy tail forms. The dynamical blueshift roughly compensates the gravitational redshift just at $l_\infty \sim 0.4$. A typical dynamically Comptonized spectrum is shown in Figure 4 for $l_\infty = 0.9$. The spectral shape is essentially Planckian up to energies ~ 20 keV and then becomes a power law with spectral index $\alpha \simeq 3.4$. We wish to stress that low- and high-luminosity models have different spectral properties because the former are everywhere optically thin (or at most marginally thick) while the latter do have an optically thick inner region. The fact that $(\tau v)_*$ is more or less the same for all the solutions does not contradict the previous statement. In fact, from the analysis of Payne & Blandford it follows that τv is the important parameter for dynamical Comptonization, but it should be taken into account that their results were obtained in the diffusion limit, that is to say, in the hypothesis of very large scattering depth. For optically thin flows, Payne & Blandford approach does not apply at all, and one has to expect the emergent spectrum to show different features. On the other hand, when $l_\infty \gtrsim 0.4$, spectra originating from near-critical accretion onto neutron stars closely resemble those obtained by PB for spherical accretion onto black holes. PB have shown, in fact, that a monochromatic line at $\nu = \nu_0$, injected at a basis of a converging fluid flow, experiences both a drift and a broadening toward frequencies higher than ν_0, as photons propagate outward. This effect is due to repeated Thomson scatterings by the moving electrons and is intrinsically similar to first-order Fermi acceleration of cosmic rays. If the flow is characterized by a constant velocity gradient $\beta = v'/v$, the emergent number flux $N_\nu = H_\nu/h\nu$ shows a power-law, high-energy tail with spectral index

$$\alpha = -\frac{\partial \ln N_\nu}{\partial \ln \nu} = \frac{5+\beta}{2+\beta}.$$

Recently MK extended PB's analysis to an accreting flow onto a neutron star. Essentially they performed again PB's calculations, but replaced the original boundary condition with the requirement that the flux vanishes at the star surface and proved that now $\alpha = 1$, irrespective of the value of β. While the overall spectral evolution is quite similar in both cases, some important points, like the value of the final power-law index, seem to depend on the choice of the condition for the radiation field at the inner boundary. This particular aspect deserves a further comment in order to understand how our numerical solutions relate to these analytical results. Both PB and MK solved a Fokker-Planck equation for the photon occupation number, $n(t, \nu)$, $t = 3\tau v \propto R^{-1}$, looking for separable solutions of the form $n = f(t)t^{3-\beta}\nu^{-p}$. The resulting ordinary differential equation for $f(t)$ is a Kummer equation with coefficients depending both on β and p. To select the unique well-behaved physical solution, boundary conditions must be provided and here the two approaches differ because the geometry changes. While PB considered a converging flow which extends up to $R = 0$ and could require regularity for $t \to \infty$, MK were forced to use a different condition (vanishing flux) at $R = R_*$ where their integration domain terminates with a finite value of t. The two conditions at the basis of the flow produce two distinct sets of eigenvalues p_n and, since $\alpha = p_0$ if the effect is saturated, this explains the different behavior at large frequencies, although the input spectrum is a monochromatic line in both cases. Actually, in the model we are considering, the integration domain is finite, as in the MK case, so that PB's analysis

certainly does not apply; our approach, however, differs also from that of MK, because in fixing the spectrum at R_*, we have assigned only the photon input without specifying any extra constraint. In this situation we do not expect to select any countable set of eigenvalues. The emergent spectrum shows, nevertheless, a well-defined power-law tail, whose index seems to be related to the physical conditions in the region where dynamical effects become important.

In concluding, we note that, although present results refer to the radial evolution of a Planckian, the global properties of the model (drift to high frequencies and formation of a power-law tail) are largely independent of the form chosen for the input spectrum.

4. DISCUSSION

Here we consider the relevance of our models in connection with the observed spectral properties of accreting neutron stars, such as those believed to power LMXBs. In comparing our synthetic spectra with actual observations one should keep in mind the drastic simplifications introduced in the model itself. We have considered a unique component, a dynamically Comptonized blackbody, and in treating radiative transfer we have neglected all emission-absorption process so that, for instance, line features do not appear.

In order to be specific we shall deal with the spectral observations of Cyg X-2, which is one of the prototypes of the class of LMXBs. We refer in particular to *EXOSAT* observations of 1983, which covered the energy band 0.5–20 keV (see Chiappetti et al. 1990) and focus our attention on the observations of September 13–22. Assuming a distance of 8 kpc (Cowley, Crampton, & Hutchings 1979), the X-ray luminosity is 1.7×10^{38} ers s^{-1}, which clearly situates the source close to the Eddington limit for $M_* \sim M_\odot$. Note that Cyg X-2 is one of the few LMXBs with such a high luminosity. A good fit to the data is formally obtained by the superposition of a bremsstrahlung at 4.4 keV and a blackbody at 1.2 keV. We consider also the high-energy observations of Maurer et al. (1982), obtained during a balloon flight in 1976 May, which detected the source in the 18–60 keV range, with the low-energy point at a level comparable to that of the *EXOSAT* observations. The high-energy count rate is well fitted by a power law of spectral index 2.8 ± 0.7. As mentioned above, a useful tool for studying the X-ray spectral properties of LMXBs are the intensity-color and color-color diagrams. Cyg X-2 was, in fact, the first source for which the constancy of the hardness ratio with respect to the intensity was discovered (Branduardi et al. 1980). This rather puzzling behavior, together with the characteristic Z-shaped track on the X-ray color-color plot, is shared by many other LMXBs; more details can be found, e.g., in Hasinger (1987) and references therein. In Figure 5 we have plotted the observations of Chiappetti et al. and Maurer et al. (errors below 20 keV are $\lesssim 10\%$) together with the computed spectrum for the model with $l_\infty = 0.9$, while a typical intensity-color plot for Cyg X-2, taken again from Chiappetti et al., is shown in Figure 6. The color is defined as the ratio of the number counts in the 6–17 and 3–6 keV bands while the intensity refers to the count rate in the 1–17 keV range.

A comparison of the synthetic spectrum with the observed one (see Fig. 5) clearly indicates that our model cannot describe the number counts in the entire energy range because it exhibits a definite photon deficit at low frequencies. However, the flux energy distribution above 10 keV is a steep power law and it is well fitted by the model; the computed spectral index,

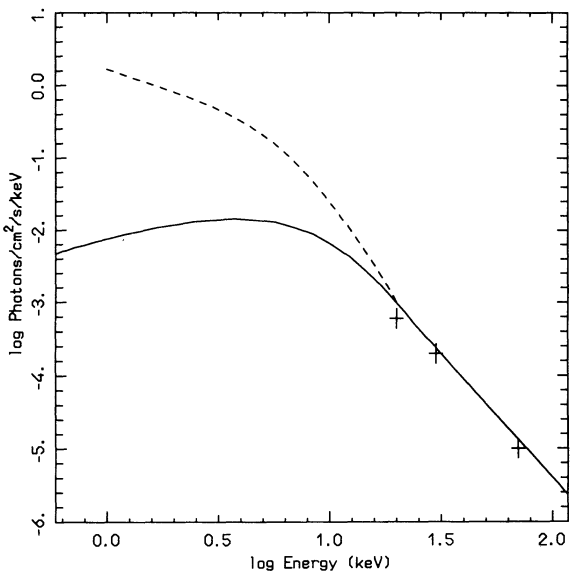

FIG. 5.—The spectrum of Cyg X-2 in the 1–60 keV range. The dotted line is the best fit to the data of Chiappetti et al., crosses refer to the observations of Maurer et al., and the solid line is the model spectrum for $l_\infty = 0.9$.

$\alpha \simeq 3.4$, is, in fact, consistent within the large uncertainties with the observed one.

The intensity-color diagram for our solutions is plotted in Figure 7. As can be seen, for luminosities $l_\infty < 0.4$ the count rate in the 1–17 keV band increases, while, for $l_\infty > 0.4$, it starts to (slowly) decrease, because the spectrum becomes harder and the total number of photons in the interval 1–17 keV becomes lower. This contrasts with the nearly linear dependence of the hardening ratio on the total luminosity (see Table 1). The turning point in the diagram corresponds to the model with $l_\infty \simeq 0.4$ which is the value of the luminosity at which the count rate is maximum. We note that the existence of an anti-

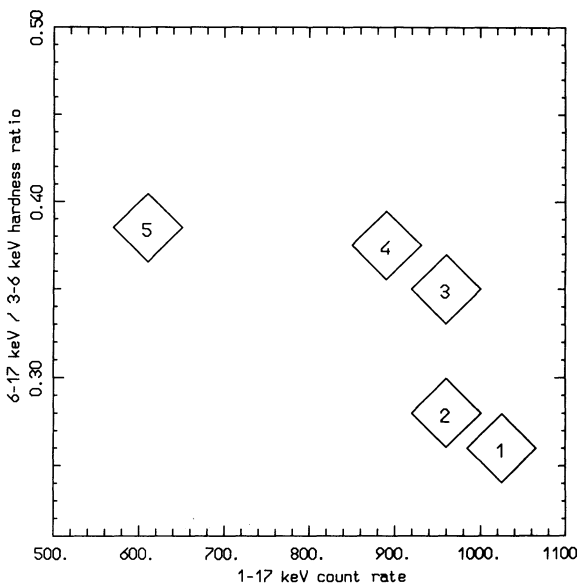

FIG. 6.—Hardness ratio vs. count rate for Cyg X-2, as from Chiappetti et al.; diamonds mark the areas covered by five different groups of observations.

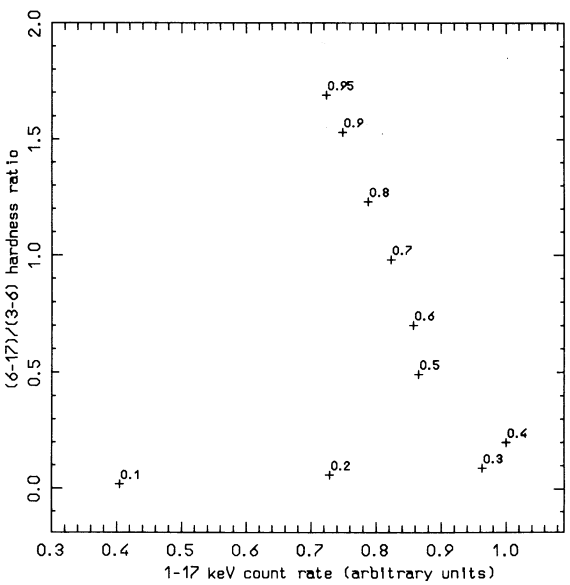

FIG. 7.—Same as in Fig. 6 for our models; each point is labeled by the value of l_∞ (see also Table 1).

correlation branch in the intensity-color diagram for our solutions is entirely due to dynamical effects. In the absence of bulk motion Comptonization, in fact, the spectrum remains Planckian and drifts to higher frequencies for increasing l_∞ just because $T_* \propto l_\infty^{1/4}$; the gravitational redshift does not enter in these considerations being the same for all the models. It can be easily checked that a Planckian spectrum produces always a positive intensity-hardness correlation when temperature is increased. The turning point appears only when dynamical effects start to be important; in this case the mean photon frequency $\bar{\nu} \propto f_b$, where $f_b > 1$ is the dynamical blueshift factor, and, as luminosity approaches L_E, f_b can become considerably large causing a decrease in the count rate, while colors continue to increase because the spectrum becomes harder.

If we explain the X-ray variability of LMXBs in terms of a time varying accretion rate, the turning point present in the intensity-color diagrams of some LMXBs (see, e.g., van der Klis 1990) bears some resemblance to the behavior of our solutions. In this respect one is tempted to interpret observations 1, 2 and 4, 5 for Figure 6 in the same terms, as corresponding to the models with luminosities in the range 0.4–0.5 of Figure 7.

In conclusion, although the simple model considered here cannot describe the overall X-ray emission of Cyg X-2, since the computed spectrum shows an evident deficit of photons at low frequencies, we find that dynamical effects due to bulk gas motion (drift to high frequencies and formation of a power law tail) may be an important ingredient to explain some of the observed spectral properties of neutron stars accreting close to the Eddington limit. The construction of a more complete model which takes into account also for emission processes in the infalling gas in addition to photons produced at the star surface is presently under consideration.

REFERENCES

Blandford, R. D., & Payne, D. G. 1981a, MNRAS, 194, 1033
———. 1981b, MNRAS, 194, 1041
Branduardi, G., Kylafis, N. D., Lamb, D. Q., & Mason, K. O. 1980, ApJ, 235, L153
Chiappetti, L., et al. 1990, ApJ, 361, 596
Colpi, M. 1988, ApJ, 326, 223
Cowley, A. P., Crampton, D., & Hutchings, J. B. 1979, ApJ, 231, 539
Hasinger, G. 1987, in IAU Symp. 125, The Origin and Evolution of Neutron Stars, ed. D. J. Helfand & J.-H. Huang (Dordrecht: Reidel), 333
Maraschi, L., Reina, C., & Treves, A. 1974, A&A, 35, 389
———. 1978, A&A, 66, 99
Mastichiadis, A., & Kylafis, N. D. 1992, ApJ, 384, 136
Matt, G., Costa, E., Dal Fiume, D., Dusi, W., Frontera, F., & Morelli, E. 1990, ApJ, 355, 468
Maurer, G. S., Johnson Neil, W., Kurfess, J. D., & Strickman, M. S. 1982, ApJ, 254, 271
Mihalas, D., Kusnaz, P. B., & Hummer, D. G. 1976, ApJ, 206, 515
Miller, G. S. 1990, ApJ, 356, 572
Nobili, L., Turolla, R., & Zampieri, L. 1991, ApJ, 383, 250
———. 1993, ApJ, 404, 686
Park, M.-G., & Miller, G. S. 1991, ApJ, 371, 708
Payne, D. G., & Blandford, R. D. 1981, MNRAS, 196, 781
Thorne, K. S. 1981, MNRAS, 194, 439
Turolla, R., & Nobili, L. 1988, MNRAS, 235, 1273
Turolla, R., Nobili, L., & Zampieri, L. 1993, preprint
van der Klis, M. 1989, ARA&A, 27, 517
———. 1990, in Neutron Stars: Theory and Observations (Dordrecht: Kluwer), 319.